Title: Parallel genetic excisions of the cardiac troponin I N-terminal extension in tachycardic mammals

Authors: William Joyce[1,2]*, Kai He[3], David Bogomolny[4], Jiuyong Xie[5], Mark S. Springer[6], Anthony V. Signore[4†], Kevin L. Campbell[4]*

Affiliations:

[1]Department of Biology - Zoophysiology, Aarhus University, Aarhus C, Denmark

[2]Division of Cardiovascular Sciences, Faculty of Biology, Medicine and Health, The University of Manchester, Manchester, UK

[3]Key Laboratory of Conservation and Application in Biodiversity of South China, School of Life Sciences, Guangzhou University, Guangzhou, Guangdong, China

[4]Department of Biological Sciences, University of Manitoba, Winnipeg, Manitoba, Canada

[5]Department of Physiology and Pathophysiology, University of Manitoba, Winnipeg, Manitoba, Canada

[6]Department of Evolution, Ecology and Organismal Biology, University of California, Riverside, Riverside, United States

*corresponding authors: william.joyce@bio.au.dk (W.J.), kevin.campbell@umanitoba.ca (K.L.C.)

[†]present address: National Centre for Foreign Animal Disease, Winnipeg, Manitoba, Canada

Abstract: Cardiac troponin I (cTnI) contains a N-terminal extension harboring protein kinase A targets ($Ser_{23/24}$), which are phosphorylated during ß-adrenergic stimulation to increase cardiomyocyte relaxation rate. Here, we show that exon 3 of *TNNI3*, encoding most of the cTnI N-terminal extension including $Ser_{23/24}$, was pseudoexonized multiple times in shrews and moles to mimic $Ser_{23/24}$ phosphorylation without adrenergic stimulation, thus facilitating the evolution of exceptionally high resting heart rates (>1100 beats/minute). Cardiac transcriptomes further reveal alternative splicing of *TNNI3* exon 3 in two distantly related bat families, thereby representing an intermediate state preceding the genomic assimilation of exon 3 skipping. As human *TNNI3* may similarly be amenable to exon 3 alternative splicing, our results offer a new approach to restore diastolic function in chronic heart failure patients.

One-Sentence Summary: Shrews and moles independently evolved a truncated cardiac troponin I to facilitate rapid heart rates without chronic adrenergic stimulation.

Main Text:

Cardiac contraction is triggered when rising cytosolic Ca^{2+} binds to troponin (Tn) in the sarcomere which, by shifting tropomyosin, allows the formation of force-generating actin-myosin crossbridges (*1*). Thus, troponin, a trimeric complex of TnC, TnI and TnT subunits, plays a pivotal role in excitation-contraction coupling, and dysregulation or mutations in troponin subunits are associated with various cardiomyopathies and heart failure (*2–6*).

In mammals, the *TNNI3* gene encodes cardiac TnI (cTnI), which is differentiated from skeletal muscle troponin I paralogs (*TNNI1* and *TNNI2*) by the presence of a ~32 amino acid N-terminal extension that plays an essential regulatory role during adrenergic stimulation (*7–12*). In the unphosphorylated state, the N-terminal extension of cTnI interacts with cTnC to increase myofilament Ca^{2+} sensitivity (*10*). However, the N-terminal extension harbors two serine residues ($Ser_{23/24}$) that are protein kinase A (PKA) substrates. Increased adrenergic stimulation during exercise or stress (*2*, *13*) induces PKA phosphorylation of $Ser_{23/24}$, thereby abolishing the TnI-TnC protein-protein interaction (*10*, *14*) and decreasing myofilament Ca^{2+} affinity (*15*). Accordingly, this process accelerates dissociation of Ca^{2+} during diastole and increases the rate of cardiomyocyte relaxation (*12*, *16*, *17*), which is essential for preserving adequate cardiac filling at elevated heart rates concomitantly driven by adrenergic stimulation (*12*, *18*, *19*). As shown in transgenic mice, truncation of the cTnI N-terminal extension mimics the effect of PKA phosphorylation (*20*, *21*) and benefits diastolic cardiac performance, particularly during aging (*9*) and deficient ß-adrenergic signaling (*22*). N-terminal truncation of cTnI has accordingly been proposed as a potential target for the treatment of heart failure (*9*, *21–23*), when cTnI phosphorylation is often impaired due to $ß_1$-adrenergic receptor desensitization (*5*, *6*, *24*).

The coding sequence of the cTnI N-terminal extension is highly conserved among eutherian mammals (*11*, *25*). However, we predicted modifications of this region could reveal evolutionary adaptation in clades with exceptionally high heart rates such as the superorder Eulipotyphla, which houses shrews (family Soricidae), the lineage with the highest known heart rates amongst mammals (up to 1500 beats min^{-1}) (*26–31*).

Genetic excision of the cTnI N-terminal extension evolved independently in shrew and mole lineages

We first collected and manually annotated *TNNI3* coding sequences from 11 eulipotyphlan species (four shrews, one hedgehog, five moles, one solenodon) using NCBI GenBank (Data S1). These data provided initial evidence for loss/inactivation of the regulatory N-terminal region (including of $Ser_{23/24}$) encoded by exon 3 (representing an 87 bp in-frame deletion) in shrews and most moles (family Talpidae). Linear genomic sequence comparisons illustrate that while the intronic region upstream of exon 3 is intact in shrews (Figure 1A), the sequence corresponding to exon 3 is unrecognizable, providing strong evidence this exon was inactivated in the common ancestor of Soricidae. By contrast, the sequence of this exon is present in moles (Figure 1B), though exhibited splice site mutations and/or frameshift indels in four of the five species initially examined. Surprisingly, exon 3 of the Pyrenean desman (*Galemys pyrenaicus*), which is nested within the mole clade (*32*, *33*) is intact, *i.e.* it exhibits no frameshift indels, premature stop codons, or splice site mutations and retains the conceptual presence of $Ser_{23/24}$.

To extend taxon sampling and verify this unexpected pattern of N-terminal truncation in Eulipotyphla, we next assembled *TNNI3* mRNA sequences from 21 eulipotyphlan species via direct cDNA sequencing (n=5), *de novo* transcriptome assembly (n=13), and/or mining of

publicly available (*n*=3) cardiac transcriptomes (Data S1). These data together confirm that exon 3, encoding the majority of the characteristic N-terminal extension, is not expressed in any of the shrews and moles examined, including, unexpectedly, the Pyrenean desman (Figure 2A).

To confirm the expression of the truncated protein as predicted from genomic and mRNA sequences, Western blots were performed with cardiac extracts from two shrews (greater white-toothed shrew, *Crocidura russula*; Eurasian pygmy shrew, *Sorex minutus*), two moles (European mole, *Talpa europaea*; Pyrenean desman, *G. pyrenaicus*), the European hedgehog (*Erinaceus europaeus*), and the well-characterized wild-type mouse (*Mus musculus*). We employed a TnI antibody that targets a region of the protein outside of the N-terminal extension that has previously been used to detect diverse TnI isoforms from a broad range of vertebrate species (*7*). These Western blots confirmed the cTnI protein expressed in shrew and mole/desman hearts was of a lower molecular mass (~24 kDa) than in mouse and hedgehog (~29 kDa) (Figures 2B and S1A). The European mole protein exhibited a marginally higher molecular mass than shrew and desman cTnI, which can be attributed to a four amino acid extension at the C-terminus (see full sequences in Data S1).

We additionally treated protein extracts from each species with PKA (recombinant catalytic subunit) *in vitro* and performed Western blots to detect $Ser_{23/24}$ phosphorylated cTnI. As expected, only the hedgehog and mouse exhibited bands that were co-localized with cTnI (Figure 2B), reaffirming that the cTnI protein of shrews and moles lacks the N-terminal extension PKA phosphorylation sites. We subsequently performed Western blots using an antibody that detects all phosphorylated PKA substrates ("RRXS*/T*") on the same PKA-treated extracts. This antibody also detected strong bands in hedgehog and mouse at ~29 kDa, consistent with cTnI, but did not reveal PKA phosphorylated proteins in the shrew or mole species at the expected location of cTnI (Figure S1B). This general PKA substrate antibody did, however, detect a range of other (unidentified) PKA substrates in moles and shrews (Figure S1B), indicating that these species have undergone a selective loss of cTnI phosphorylatability, as opposed to showing a generalized lack of responsiveness to PKA.

In contrast to shrews and moles, genomic, mRNA, and/or protein evidence together support the presence of the cTnI N-terminal extension PKA phosphorylation residues in all four erinaceid (hedgehog and gymnure) species investigated (*Atelerix albiventris*, *E. europaeus*, *Neohylomys hainanensis*, and *Neotetracus sinensis*) (Figure 2A; Data S1). As phylogenomic data indicate a robust sister relationship between erinaceids and shrews (*32*, *33*), our results strongly support the independent genetic excision of *TNNI3* exon 3 in the shrew and mole lineages (Figure 2A). The evolutionary deletion of *TNNI3* exon 3 is analogous to N-terminal truncation previously characterized in transgenic mice (*9*, *21*), and likely contributes to improving diastolic performance that augments ventricular filling and hence supported the evolution of exceptionally high resting heart rates in shrews (up to 1130 bpm (*26*, *27*)). It was initially surprising to find a genetically abbreviated N-terminal extension in mole hearts, given that fossorial European moles (*T. europaea*) have relatively slow heart rates for their body mass (~160 beats min^{-1} under anaesthesia (*34*)). However, strictly fossorial Talpini and Scalopini moles (which include the genera *Talpa* and *Scalopus*, respectively) evolved convergently from small, ambulatory, and presumably highly active shrew-like ancestors (*32*, *33*). Indeed, American shrew-moles (*Neurotrichus gibbsii*) and star-nosed moles (*Condylura cristata*), which are nested between the above two fossorial clades (*32*), exhibit high mass-specific metabolic rates that are comparable to soricid shrews (*35*, *36*). Thus, it is most plausible that the N-terminus of cTnI was independently truncated in small, shrew-like mole ancestors of these two fossorial lineages under much the same selective pressures as in shrews, *i.e.* to support extreme cardiac and metabolic demands.

To better elucidate the evolutionary and genomic underpinnings of exon 3 inactivation within the talpid family, we next sequenced the *TNNI3* N-terminal region (using genomic DNA) from three additional mole species (*Uropsilus gracilis*, *Urotrichus talpoides,* and *Desmana moschata*). These data reveal that, like its close relative *G. pyrenaicus*, the Russian desman (*D. moschata*) retains an intact exon 3 that is potentially functional/expressed (Figure 1B). By contrast, representative species from the remaining five talpid clades (*Talpa*, *Condylura*, *Urotrichus*, *Scalopus*, *Uropsilus*) all exhibit inactivating mutations in exon 3 that are hallmarks of pseudoexonization (Figure S2). For example, the exon 3 donor and acceptor splice sites are intact in Scalopini moles and Urotrichini shrew moles, though their exons have been functionally inactivated by frameshift insertions/deletions. *Uropsilus* and *Condylura*, in turn, have independently accumulated acceptor splice site mutations and frameshift deletions. Finally, Talpini moles exhibit a 10-bp coding sequence frameshift deletion and a 26-bp deletion that encompasses the acceptor splice site (Figure S2). The central placement of desmans within Talpidae (*32*) implies the loss of regulatory cTnI phosphorylation must have occurred a minimum of three times in the common ancestors of: (1) shrew-like moles (*Uropsilus*), (2) Scalopini moles (*Scalopus*), and (3) a clade that includes Talpini moles (*Talpa*), star-nosed moles (*Condylura*), and shrew moles (*Urotrichus*) (Figure 2A). However, as none of the above talpid lineages share common inactivating mutations of exon 3 (Figure S2), the N-terminal extension of cTnI appears to have been independently disrupted in *Uropsilus*, *Scalopus*, *Talpa*, *Condylura*, and *Urotrichus*.

Desman *TNNI3* exon 3 evolved under purifying selection and may be alternatively spliced

Given our finding that exon 3 is inactivated in shrews and most moles but not desmans, we performed selection analyses with codeml (*35*) and RELAX (*55*) to probe the molecular evolutionary history of *TNNI3* in these eulipotyphlans versus other placental mammals. First, we examined complete protein-coding sequences, minus exon 3, for a data set comprised of 48 taxa including 16 shrews and eight moles (Figure S3). This allowed us to test the hypothesis that exons 1, 2, and 4-8 have remained under purifying selection in shrew and mole taxa with pseudoexonized exon 3 sequences. The results of these analyses confirm that the *TNNI3* gene (with exon 3 removed) has evolved under strong purifying selection within Eutheria including moles and shrews (ω=0.038 to 0.0669 with different codon frequency models; Figure S3; Data S2a). Statistical tests reject the hypothesis that ω values in shrews and non-desman moles are different from those in other placental mammals (Data S2a,c). Further, ω values for *TNNI3* coding sequences (minus exon 3) for different shrew and mole branches with inactivating mutations in exon 3 range from 0.0001 to 0.1846 and are fully consistent with purifying selection (Data S2b). By contrast, ω values for pseudoexonic branches of exon 3 in non-desman moles are under relaxed selection (ω =0.867) relative to non-talpid mammals (ω=0.142) (p=0.000), as may be expected for pseudoexonic sequences (Figure 3, Figure S4, DataS2d). In the case of desmans, we hypothesized that the coding sequences for exon 3 may be evolving under neutral selection—like in other talpid species—given the absence of direct evidence for exon 3 expression in mature mRNA or heart Western blots (Figure 2). To test this hypothesis, we compared ω values in Desmanini to non-talpid placental mammals. The ω value for desmans (0.490) is elevated, but not significantly (p=0.07) different from the value in other mammals (0.121) with an intact copy of exon 3 (Figure S5, Data S2e).

Importantly, results of the selection analyses are consistent with the hypothesis that exon 3 of desmans could be variably expressed (*i.e.* via alternative exon splicing). To further examine the potential for *TNNI3* exon 3 alternative splicing in this clade, the strengths of the upstream

(intron 2) 3′ acceptor splice site and downstream (intron 3) 5' donor splice site were assessed using maximum entropy modelling (*37*) with comparisons to representative outgroup species with intact exon 3 sequences (Figure 4; Data S3). The splice strengths (MaxEnt scores) were similar across all species for exon 2 and exon 4 upstream and downstream splice sites. However, only desmans exhibited drastically reduced upstream 3' splice site strength for exon 3 (Figure 4B). The *TNNI3* exon 3 downstream 5' splice site, by contrast, was highly conserved and retained a comparably high splice strength score relative to the other eulipotyphlan species (solenodons and erinaceids) (Fig. 4E). Notably, this combination of a low 3' splice score and a high 5' splice score renders exon 3 of desmans liable to alternative splicing (*38*). This conclusion is significant in that it conflicts with the prevailing consensus that *TNNI3* does not undergo alternative exon splicing in vertebrates (*11*, *39*). Although cTnI protein assays from five *G. pyrenaicus* specimens failed to demonstrate alternative exon splicing in cardiac tissue (Figure S1C), it remains possible that exon 3 is expressed in the heart under certain circumstances (*i.e.* developmentally or seasonally). Alternatively, the human protein atlas provides direct evidence for cTnI expression in testis tissue (specifically, developing spermatids/spermatocytes; https://www.proteinatlas.org/ENSG00000129991-TNNI3/tissue). Indeed, publicly available RNA-seq data from *T. occidentalis* testis tissue (*40*) confirms this expression profile in moles, thus also opening the possibility for *TNNI3* exon 3 translation in this organ of desmans. In addition to alternative exon 3 splicing in desmans, we also found transcriptomic evidence for alternative donor splice sites in exon 4 (*Sorex hosonoi*) and exon 7 in numerous shrew species (Data S1), suggesting that *TNNI3* alternative splice sites may be prevalent within Eulipotyphla.

TNNI3 exon 3 is alternatively spliced in bats

Like shrews, bats (family Chiroptera) are able to sustain high metabolic rates (*41*) with some species exhibiting maximal heart rates up to 1000 beats min^{-1} (*42*, *43*). While genomic data show that the phosphorylatable cTnI N-terminal extension of bats is intact (Figure 2A; Figure 3; Data S1), our analysis of cardiac cTnI transcripts from six chiropteran species unambiguously demonstrates alternative splicing of exon 3 in at least two distantly related families (Phyllostomidae, suborder Yangochiroptera, and Hipposideridae, suborder Yinpterochiroptera) (Figure S6). Importantly, this finding offers a plausible scenario for the pattern of exon 3 pseudoexonization in shrews and moles. Specifically, the ability to alternatively splice exon 3—possibly still present in desmans—may have an ancient evolutionary origin in the common ancestors of both shrews and moles. The presence of intact exon 3 donor and acceptor splice sites several extant mole lineages (*i.e. Scalopus* and *Urotrichus*) provides evidence that the truncated N-terminal region of the protein later became fixed via the genetic assimilation of exon 3 excision in pre-mRNA transcripts, and was followed by the independent degeneration of this coding region in each of the five non-desman mole clades (Figure 2; Figure S2). Surprisingly, both species of bats shown to be capable of alternatively splicing, *Hipposideros armiger* and *Artibeus jamaicensis* (Figure S6), exhibit high 3' and 5' MaxEnt splice site scores (Figure 4), in favor of only exon inclusion (*38*). This suggests that exon 3 alternative splicing must be mainly dependent on *trans*-acting factors in these species (*44*, *45*).

We hypothesize that the genomic retention of exon 3 in Chiroptera may in part be related to the ability of many bat species to enter into seasonal hibernation. Low body temperature, as experienced during hibernation, reduces myofilament Ca^{2+} sensitivity (*46*), potentially leading to cardiac asystole. However, in compensation, some hibernating mammals are able to increase myofilament Ca^{2+} affinity (*47*). This is likely attributable, at least in part, to the effects of reduced adrenergic stimulation (*48*) and a corresponding reduction of cTnI phosphorylation. In

this situation, the non-phosphorylated N-terminal extension would play an essential role to safeguard myofilament Ca^{2+} sensitivity. Although the ability to enter short-term torpor is widespread among crociduran (white-toothed) shrews (*49*), no other eulipotyphlan lineage apart from hedgehogs (which express the phosphorylatable N-terminal extension) is known to exploit true hibernation. This observation suggests that the loss of *TNNI3* exon 3 could be a historical contingency that prevents moles and shrews from partaking in hibernation as a seasonal energy conservation strategy.

Tachycardic mammals reveal new pathways to therapeutically target cTnI truncation

Reduced cTnI phosphorylation, leading to increased Ca^{2+} affinity of the troponin complex, is a hallmark of chronic heart failure and may contribute to diastolic cardiac dysfunction (*5*, *6*, *24*). However, the transgenic overexpression of N-terminal truncated cTnI in mice has been shown to mimic the effect of PKA activation in reducing myofilament Ca^{2+} sensitivity (*9*, *21*). As such, removal of the N-terminal extension of cTnI has been proposed as a potential treatment to restore diastolic function during heart failure (*9*, *21–23*). Crucially, it provides a mechanism to increase the rate of relaxation (and hence end-diastolic volume) in the absence of chronic adrenergic stimulation (*9*), the latter of which is known to lead to $ß_1$-adrenergic receptor desensitization and cardiac hypertrophy during the progression of heart failure (*50*). Although generated by a different mechanism—pseudoexonization of exon 3 in shrews and moles *versus* insertion of an artificial translation initiation codon in transgenic mice (*21*)—the truncated N-terminal cTnIs share a strikingly close resemblance, being of virtually equal length (one amino acid fewer in shrew and mole N-termini) and sharing a number of highly conserved amino acids (Figure S7). The capacity for alternative splicing of exon 3, evidenced in bats and strongly implicated in desmans, provides a potential reversible strategy for exon exclusion in mature human *TNNI3* transcripts. Although *TNNI3* exon 3 was not known to be alternatively spliced in mammals prior to this study (*11*, *51*), and we can find no evidence that it is ever excluded in human *TNNI3*, our maximum entropy modelling suggests exon 3 has relatively low splice site strength scores even in humans (Figure 4B,E,H). These results suggest that *TNNI3* may be amenable to alternative splicing in our own species (*38*). By beginning to uncover the mechanism of exon 3 alternative splicing in diverse species such as desmans and bats, our study lays the foundations to explore how exon 3 excision might be therapeutically induced during diastolic heart failure in humans. Together, by studying the hearts of small mammals with exceptionally high heart rates (*26*), we have also shown that nature realized the solution to habitually accelerate diastolic relaxation—by genetic truncation of cTnI—long before modern biomedicine.

References

1. D. M. Bers, Cardiac excitation–contraction coupling. *Nature*. **415**, 198–205 (2002).

2. J. van der Velden, G. J. M. Stienen, Cardiac disorders and pathophysiology of sarcomeric proteins. *Physiol. Rev.* **99**, 381–426 (2019).

3. S. Morimoto, Sarcomeric proteins and inherited cardiomyopathies. *Cardiovasc. Res.* **77**, 659–666 (2008).

4. P. M. Hwang, B. D. Sykes, Targeting the sarcomere to correct muscle function. *Nat. Rev. Drug Discov.* **14**, 313–328 (2015).

5. P. J. M. Wijnker, A. M. Murphy, G. J. M. Stienen, J. van der Velden, Troponin I phosphorylation in human myocardium in health and disease. *Neth. Heart J.* **22**, 463–469 (2014).

6. G. S. Bodor, A. E. Oakeley, P. D. Allen, D. L. Crimmins, J. H. Ladenson, P. A. Anderson, Troponin I phosphorylation in the normal and failing adult human heart. *Circulation*. **96**, 1495–1500 (1997).

7. W. Joyce, D. M. Ripley, T. Gillis, A. C. Black, H. A. Shiels, F. G. Hoffmann, A revised perspective on the evolution of troponin I and troponin T gene families in vertebrates. *Genome Biol. Evol.* **15**, evac173 (2023).

8. H. E. Salhi, V. Shettigar, L. Salyer, S. Sturgill, E. A. Brundage, J. Robinett, Z. Xu, E. Abay, J. Lowe, P. M. L. Janssen, J. A. Rafael-Fortney, N. Weisleder, M. T. Ziolo, B. J. Biesiadecki, The lack of Troponin I Ser-23/24 phosphorylation is detrimental to in vivo cardiac function and exacerbates cardiac disease. *J. Mol. Cell. Cardiol.* (2023), doi:10.1016/j.yjmcc.2023.01.010.

9. B. J. Biesiadecki, K. Tachampa, C. Yuan, J.-P. Jin, P. P. de Tombe, R. J. Solaro, Removal of the cardiac troponin I N-terminal extension improves cardiac function in aged mice. *J. Biol. Chem.* **285**, 19688–19698 (2010).

10. P. M. Hwang, F. Cai, S. E. Pineda-Sanabria, D. C. Corson, B. D. Sykes, The cardiac-specific N-terminal region of troponin I positions the regulatory domain of troponin C. *Proc. Natl. Acad. Sci. U. S. A.* **111**, 14412–14417 (2014).

11. J.-J. Sheng, J.-P. Jin, TNNI1, TNNI2 and TNNI3: Evolution, regulation, and protein structure–function relationships. *Gene*. **576**, 385–394 (2016).

12. S. Marston, Recent studies of the molecular mechanism of lusitropy due to phosphorylation of cardiac troponin I by protein kinase A. *J. Muscle Res. Cell Motil.* (2022), doi:10.1007/s10974-022-09630-4.

13. D. M. Bers, Y. K. Xiang, M. Zaccolo, Whole-Cell cAMP and PKA activity are epiphenomena, nanodomain signaling matters. *Physiol. Bethesda Md*. **34**, 240–249 (2019).

14. G. Ferrières, M. Pugnière, J. C. Mani, S. Villard, M. Laprade, P. Doutre, B. Pau, C. Granier, Systematic mapping of regions of human cardiac troponin I involved in binding to cardiac troponin C: N- and C-terminal low affinity contributing regions. *FEBS Lett.* **479**, 99–105 (2000).

15. J. Wattanapermpool, X. Guo, R. J. Solaro, The unique amino-terminal peptide of cardiac troponin I regulates myofibrillar activity only when it is phosphorylated. *J. Mol. Cell. Cardiol.* **27**, 1383–1391 (1995).

16. S. Yasuda, P. Coutu, S. Sadayappan, J. Robbins, J. M. Metzger, Cardiac transgenic and gene transfer strategies converge to support an important role for troponin I in regulating relaxation in cardiac myocytes. *Circ. Res.* **101**, 377–386 (2007).

17. R. Zhang, J. Zhao, A. Mandveno, J. D. Potter, Cardiac troponin I phosphorylation increases the rate of cardiac muscle relaxation. *Circ. Res.* **76**, 1028–1035 (1995).

18. W. Joyce, T. Wang, How cardiac output is regulated: August Krogh's proto-Guytonian understanding of the importance of venous return. *Comp. Biochem. Physiol. A. Mol. Integr. Physiol.* **253**, 110861 (2021).

19. S. Marston, J. R. Pinto, Suppression of lusitropy as a disease mechanism in cardiomyopathies. *Front. Cardiovasc. Med.* **9** (2023) (available at https://www.frontiersin.org/articles/10.3389/fcvm.2022.1080965).

20. L. K. Gunther, H.-Z. Feng, H. Wei, J. Raupp, J.-P. Jin, T. Sakamoto, Effect of N-terminal extension of cardiac troponin I on the Ca^{2+} regulation of ATP-binding and ADP dissociation of myosin II in native cardiac myofibrils. *Biochemistry*. **55**, 1887–1897 (2016).

21. J. C. Barbato, Q.-Q. Huang, M. M. Hossain, M. Bond, J.-P. Jin, Proteolytic N-terminal truncation of cardiac troponin I enhances ventricular diastolic function. *J. Biol. Chem.* **280**, 6602–6609 (2005).

22. H.-Z. Feng, M. Chen, L. S. Weinstein, J.-P. Jin, Removal of the N-terminal extension of cardiac troponin I as a functional compensation for impaired myocardial β-adrenergic signaling. *J. Biol. Chem.* **283**, 33384–33393 (2008).

23. H.-Z. Feng, X. Huang, J.-P. Jin, N-terminal truncated cardiac troponin I enhances Frank-Starling response by increasing myofilament sensitivity to resting tension. *J. Gen. Physiol.* **155**, e202012821 (2023).

24. A. E. Messer, A. M. Jacques, S. B. Marston, Troponin phosphorylation and regulatory function in human heart muscle: dephosphorylation of Ser23/24 on troponin I could account for the contractile defect in end-stage heart failure. *J. Mol. Cell. Cardiol.* **42**, 247–259 (2007).

25. J. F. Shaffer, T. E. Gillis, Evolution of the regulatory control of vertebrate striated muscle: the roles of troponin I and myosin binding protein-C. *Physiol. Genomics*. **42**, 406–419 (2010).

26. M. Vornanen, Maximum heart rate of soricine shrews: correlation with contractile properties and myosin composition. *Am. J. Physiol.* **262**, R842-851 (1992).

27. K. D. Jürgens, R. Fons, T. Peters, S. Sender, Heart and respiratory rates and their significance for convective oxygen transport rates in the smallest mammal, the Etruscan shrew *Suncus etruscus*. *J. Exp. Biol.* **199**, 2579–2584 (1996).

28. M. Vornanen, Basic functional properties of the cardiac muscle of the common shrew (*Sorex araneus*) and some other small mammals. *J. Exp. Biol.* **145**, 339–351 (1989).

29. Y. H. Chang, B. I. Sheftel, B. Jensen, Anatomy of the heart with the highest heart rate. *J. Anat.* **241**, 173–190 (2022).

30. P. Morrison, F. A. Ryser, A. R. Dawe, Studies on the Physiology of the Masked Shrew *Sorex cinereus*. *Physiol. Zool.* **32**, 256–271 (1959).

31. A. Nagel, The electrocardiogram of European shrews. *Comp. Biochem. Physiol. A Physiol.* **83**, 791–794 (1986).

32. K. He, T. G. Eastman, H. Czolacz, S. Li, A. Shinohara, S. Kawada, M. S. Springer, M. Berenbrink, K. L. Campbell, Myoglobin primary structure reveals multiple convergent transitions to semi-aquatic life in the world's smallest mammalian divers. *eLife*. **10**, e66797 (2021).

33. K. He, A. Shinohara, K. M. Helgen, M. S. Springer, X.-L. Jiang, K. L. Campbell, Talpid mole phylogeny unites shrew moles and illuminates overlooked cryptic species diversity. *Mol. Biol. Evol.* **34**, 78–87 (2017).

34. A. Armsby, T. Quilliam, H. Soehnle, Some observations on the ecology of the mole. *J. Zool. - J ZOOL*. **149**, 110–112 (2009).

35. K. L. Campbell, P. W. Hochachka, Thermal biology and metabolism of the American shrew-mole, *Neurotrichus gibbsii*. *J. Mammal.* **81**, 578–585 (2000).

36. K. L. Campbell, I. W. McIntyre, R. A. MacArthur, Fasting metabolism and thermoregulatory competence of the star-nosed mole, *Condylura cristata* (Talpidae: Condylurinae). *Comp. Biochem. Physiol. A. Mol. Integr. Physiol.* **123**, 293–298 (1999).

37. G. Yeo, C. B. Burge, Maximum entropy modeling of short sequence motifs with applications to RNA splicing signals. *J. Comput. Biol. J. Comput. Mol. Cell Biol.* **11**, 377–394 (2004).

38. P. J. Shepard, E.-A. Choi, A. Busch, K. J. Hertel, Efficient internal exon recognition depends on near equal contributions from the 3′ and 5′ splice sites. *Nucleic Acids Res.* **39**, 8928–8937 (2011).

39. J.-J. Sheng, J.-P. Jin, Gene regulation, alternative splicing, and posttranslational modification of troponin subunits in cardiac development and adaptation: a focused review. *Front. Physiol.* **5**, 165 (2014).

40. F. M. Real, S. A. Haas, P. Franchini, P. Xiong, O. Simakov, H. Kuhl, R. Schöpflin, D. Heller, M.-H. Moeinzadeh, V. Heinrich, T. Krannich, A. Bressin, M. F. Hartmann, S. A. Wudy, D. K. N. Dechmann, A. Hurtado, F. J. Barrionuevo, M. Schindler, I. Harabula, M. Osterwalder, M. Hiller, L. Wittler, A. Visel, B. Timmermann, A. Meyer, M. Vingron, R. Jiménez, S. Mundlos, D. G. Lupiáñez, The mole genome reveals regulatory rearrangements associated with adaptive intersexuality. *Science*. **370**, 208–214 (2020).

41. J. R. Speakman, D. W. Thomas, "Physiological ecology and energetics of bats" in *Bat Ecology*, T. Kunz, M. Fenton, Eds. (University of Chicago Press, Chicago, 2003), pp. 430–490.

42. D. K. N. Dechmann, S. Ehret, A. Gaub, B. Kranstauber, M. Wikelski, Low metabolism in a tropical bat from lowland Panama measured using heart rate telemetry: an unexpected life in the slow lane. *J. Exp. Biol.* **214**, 3605–3612 (2011).

43. M. T. O'Mara, M. Wikelski, C. C. Voigt, A. Ter Maat, H. S. Pollock, G. Burness, L. M. Desantis, D. K. Dechmann, Cyclic bouts of extreme bradycardia counteract the high metabolism of frugivorous bats. *eLife*. **6**, e26686 (2017).

44. C. Zhu, Z. Chen, W. Guo, Pre-mRNA mis-splicing of sarcomeric genes in heart failure. *Biochim. Biophys. Acta*. **1863**, 2056–2063 (2017).

45. M. Llorian, C. W. J. Smith, Decoding muscle alternative splicing. *Curr. Opin. Genet. Dev.* **21**, 380–387 (2011).

46. S. M. Harrison, D. M. Bers, Influence of temperature on the calcium sensitivity of the myofilaments of skinned ventricular muscle from the rabbit. *J. Gen. Physiol.* **93**, 411–428 (1989).

47. B. Liu, L. C. Wang, D. D. Belke, Effects of temperature and pH on cardiac myofilament Ca^{2+} sensitivity in rat and ground squirrel. *Am. J. Physiol.* **264**, R104-8 (1993).

48. W. K. Milsom, M. B. Zimmer, M. B. Harris, Regulation of cardiac rhythm in hibernating mammals. *Comp. Biochem. Physiol. A. Mol. Integr. Physiol.* **124**, 383–391 (1999).

49. J. Taylor, "Evolution of energetic strategies in shrews" in (1998), pp. 309–346.

50. S. Engelhardt, L. Hein, F. Wiesmann, M. J. Lohse, Progressive hypertrophy and heart failure in β1-adrenergic receptor transgenic mice. *Proc. Natl. Acad. Sci.* **96**, 7059–7064 (1999).

51. M. Rasmussen, J.-P. Jin, Troponin variants as markers of skeletal muscle health and diseases. *Front. Physiol.* **12**, 747214 (2021).

52. R. W. Meredith, J. E. Janečka, J. Gatesy, O. A. Ryder, C. A. Fisher, E. C. Teeling, A. Goodbla, E. Eizirik, T. L. L. Simão, T. Stadler, D. L. Rabosky, R. L. Honeycutt, J. J. Flynn, C. M. Ingram, C. Steiner, T. L. Williams, T. J. Robinson, A. Burk-Herrick, M. Westerman, N. A. Ayoub, M. S. Springer, W. J. Murphy, Impacts of the Cretaceous Terrestrial Revolution and KPg txtinction on mammal diversification. *Science*. **334**, 521–524 (2011).

53. S. F. Altschul, T. L. Madden, A. A. Schäffer, J. Zhang, Z. Zhang, W. Miller, D. J. Lipman, Gapped BLAST and PSI-BLAST: a new generation of protein database search programs. *Nucleic Acids Res.* **25**, 3389–3402 (1997).

54. M. J. Sullivan, N. K. Petty, S. A. Beatson, Easyfig: a genome comparison visualizer. *Bioinforma. Oxf. Engl.* **27**, 1009–1010 (2011).

55. J. O. Wertheim, B. Murrell, M. D. Smith, S. L. Kosakovsky Pond, K. Scheffler, RELAX: Detecting relaxed selection in a phylogenetic framework. *Mol. Biol. Evol.* **32**, 820–832 (2015).

56. S. L. K. Pond, S. D. W. Frost, S. V. Muse, HyPhy: hypothesis testing using phylogenies. *Bioinformatics*. **21**, 676–679 (2005).

57. R. W. Meredith, J. Gatesy, W. J. Murphy, O. A. Ryder, M. S. Springer, Molecular decay of the tooth gene enamelin (ENAM) mirrors the loss of enamel in the fossil record of placental mammals. *PLOS Genet.* **5**, e1000634 (2009).

58. A. J. Sabucedo, K. G. Furton, Estimation of postmortem interval using the protein marker cardiac Troponin I. *Forensic Sci. Int.* **134**, 11–16 (2003).

59. Y. Wang, Y. Zhang, W. Hu, S. Xie, C.-X. Gong, K. Iqbal, F. Liu, Rapid alteration of protein phosphorylation during postmortem: implication in the study of protein phosphorylation. *Sci. Rep.* **5**, 15709 (2015).

Acknowledgments: We are grateful to Jorge Gonzales Esteban for providing Pyrenean desman heart samples and five anonymous donors for additional tissue samples used in this study. Animal illustrations were created by Laura Cadiz, Umi Matsushita, and Carl Buell (authorization for the latter kindly provided by John Gatesy).

Funding:

Novo Nordisk Foundation grant NNF19OC0055842 (WJ)

Guangdong Natural Science Funds for Distinguished Young Scholars 2022B1515020033 (KH)

University of Manitoba Faculty of Science Undergraduate Research Award (DB)

National Sciences and Engineering Research Council (NSERC) of Canada Discovery grant RGPIN-2022-05023 (JX)

National Sciences and Engineering Research Council (NSERC) of Canada Discovery grant RGPIN-2016-06562 (KLC)

Author contributions:

Conceptualization: WJ, KLC

Methodology: WJ, KH, DB, JX, MS, AVS, KLC

Investigation: WJ, KH, DB, JX, MS, AVS, KLC

Visualization: WJ, KH, MS, KLC

Funding acquisition: WJ, KH, JX, KLC

Project administration: WJ, KLC

Supervision: KLC

Writing – original draft: WJ, KLC

Writing – review & editing: WJ, KH, DB, JX, MS, AVS, KLC

Competing interests: Authors declare that they have no competing interests.

Data and materials availability: All data are available in the main text or the supplementary materials.

Supplementary materials

Data S1 to S3

Materials and methods (Tables S1 to S2)

Figures S1-S7

References (*53-59)*

Figure legends

Figure 1. Sequence identity comparisons of the *TNNI3* gene of select eulipotyphlan mammals. (A) Linear comparisons illustrating the deletion of exon 3 (expected location denoted by open dashed boxes) in the genomes of four shrew species relative to the Pyrenean desman (*Galemys pyrenaicus*). B) Linear comparisons of four talpid mole species relative to the European hedgehog (*Erinaceus europaeus*). Coding exons are numbered and highlighted in red, while pseudoexonized (non-coding) exon 3 of moles is denoted by red open boxes. Thick black lines represent intron sequences while gaps denote missing data. Note that the sequence identity of the intact coding exons of most moles (but not the Pyrenean desman) relative to corresponding coding exons of the hedgehog are higher than that of the non-coding exon 3.

Figure 2. Cardiac troponin I (cTnI) primary structure, protein expression, and phosphorylation in eulipotyphlans (highlighted by shaded blue) and other mammals. (A) Representative mammalian N-terminal extension protein sequences determined from genome annotations and mRNA sequencing demonstrating the independent genomic excision of exon 3 in shrews and most mole species (the deleted exon is denoted by dashes). Dotted lines on the cladogram show branches reconstructed to have a pseudoexonized exon 3. Underscored sequences in italics correspond to exon 3 of desmans and *Hipposideros armiger*, which are intact and supported to exhibit alternative splicing (see text for details). Red arrows denote the protein kinase A (PKA) target residues ($Ser_{23/24}$; indicated in bold), which lowers Ca^{2+} sensitivity of the troponin complex upon phosphorylation. For full database (including 32 eulipotyphlan species) and accession information, please see Data S1. *Homo*: *H. sapiens*, human; *Mus*: *M. musculus*, house mouse; *Hipposideros: H. armiger,* great roundleaf bat; *Solenodon: S. paradoxus*, Hispaniolan solenodon; *Crocidura*: *C. indochinensis*, Indochinese shrew; *Suncus*: *S. etruscus*, Etruscan shrew; *Sorex*: *S. araneus*, common shrew; *Anourosorex*: *A. squamipes*, Chinese mole shrew; *Erinaceus*: *E. europaeus*, European hedgehog; *Neotetracus*: *N. sinensis*, shrew gymnure; *Uropsilus*: *U. nivatus*, snow mountain shrew-like mole; *Scalopus*: *S. aquaticus*, eastern mole; *Galemys*: *G. pyrenaicus*, Pyrenean desman; *Desmana*: *Desmana moschata*, Russian desman, *Urotrichus*: *U. talpoides*, Japanese shrew mole; *Condylura*: *C. cristata*, star-nosed mole; *Talpa*: *T. europaea*, European mole. (B) Western blotting of protein kinase A treated cardiac extracts from mouse and five eulipotyphlan species. The membrane was first probed for $Ser_{23/24}$ phoshorylated-cTnI, then stripped and re-probed for total cTnI. Total protein was visualised with

No-Stain Protein Labeling Reagent. *Mus*: *M. musculus*, house mouse; *Erinaceus*: *E. europaeus*, European hedgehog; *Crocidura*: *C. russula*, greater white-toothed shrew; *Sorex*: *S. minutus*, pygmy shrew; *Galemys*: *G. pyrenaicus*, Pyrenean desman; *Talpa*: *T. europaea*, European mole. For blots incorporating additional sample replicates without PKA treatment and using direct cTnI blotting, see Figure S1.

Figure 3. Phylogenetic tree and exon diagrams showing different evolutionary pressures on *TNNI3* exons in a diverse array of placental mammals as evidenced by inactivating mutations and selection analyses (ω values). *TNNI3* excluding exon 3 (black boxes) is under strong purifying selection in all placental mammals (ω=0.052, Data S2a, also see Data S2b,c). Exon 3 of all living shrews was unrecognizable (dashed red boxes), and presumably inactivated in the common ancestor of Soricidae. This exon is inactivated in all non-desman talpids (red boxes) based on the occurrence of splice site mutations and/or frameshift mutations (Figure S2), and has evolved under relaxed selection in these taxa (ω=0.87, see Data S2d for details). Exon 3 in all other mammals including desmans (green boxes) has evolved under purifying selection (ω=0.14). For complete information on the species used in the RELAX *(55)* selection analyses summarized here, refer to Figures S3-S6. Hatched boxes represent (pseudo)exons where no sequence data is available. The species tree is based on Meredith et al. (2011) (*52*) and He et al. (2021) (*32*). Abreviations, E = exon. Some images of animals by Carl Buell.

Figure 4. Maximum entropy (MaxEnt[14]) upstream (3' site of previous intron) and downstream (5' site of subsequent intron) splice site strength scoring for *TNNI3* (A) exon 2, (B) exon 3 (yellow boxes), and (C) exon 4. This analysis was conducted for desmans (*Galemys*: *G. pyrenaicus*, Pyrenean desman; *Desmana: D. moschata,* Russian desman), the only talpid moles with a putatively functional exon 3, and outgroups that also express exon 3 (*Homo*: *H. sapiens*, human; *M. musculus*, house mouse; *Hipposideros: H. armiger,* great roundleaf bat; *Artibeus*: *A. jamaicensis*, Jamaican fruit bat; *Solenodon: S. paradoxus*, Hispaniolan solenodon; *Erinaceus*: *E. europaeus*, European hedgehog; *Neohylomys*: *N. hainanensis*, Hainan moonrat). Splice site strength was well conserved and high across species for exons 2 (A, D, G) and 4 (C, F, I). However, desmans exhibited dramatically reduced 3' splice site strength for exon 3 (B), although they retained high 5' splice site strength (E), which together indicates the exon is likely capable of alternative splicing (*38*).

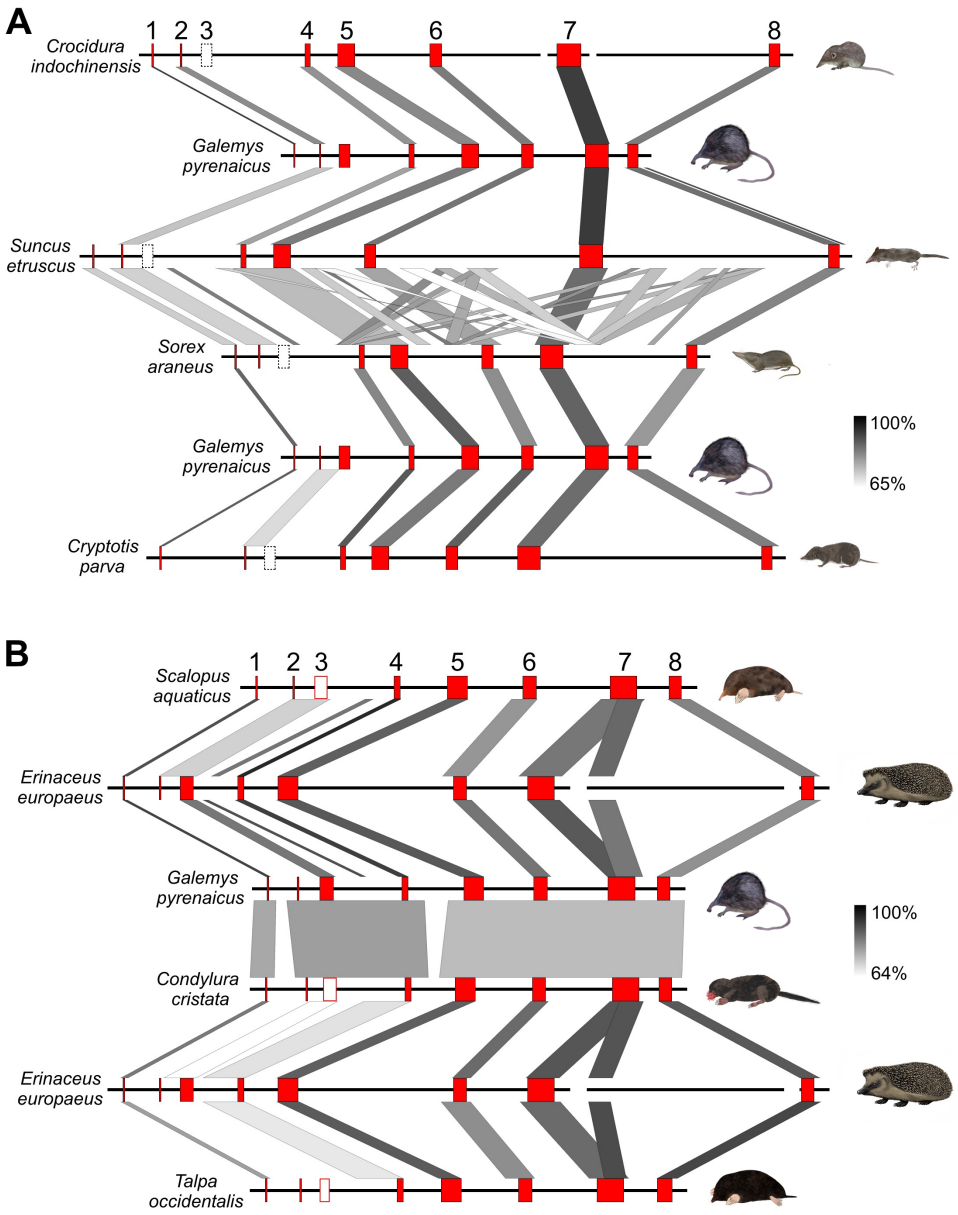

Figure 1.

5

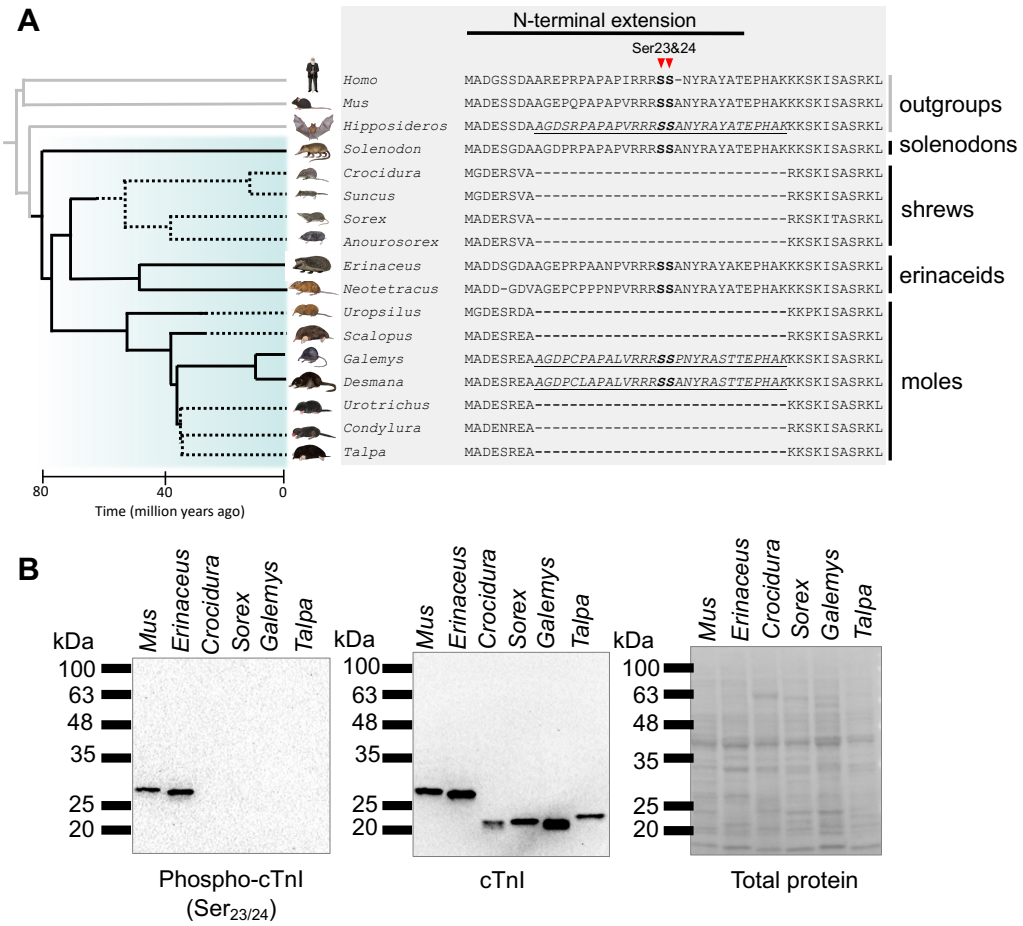

Figure 2.

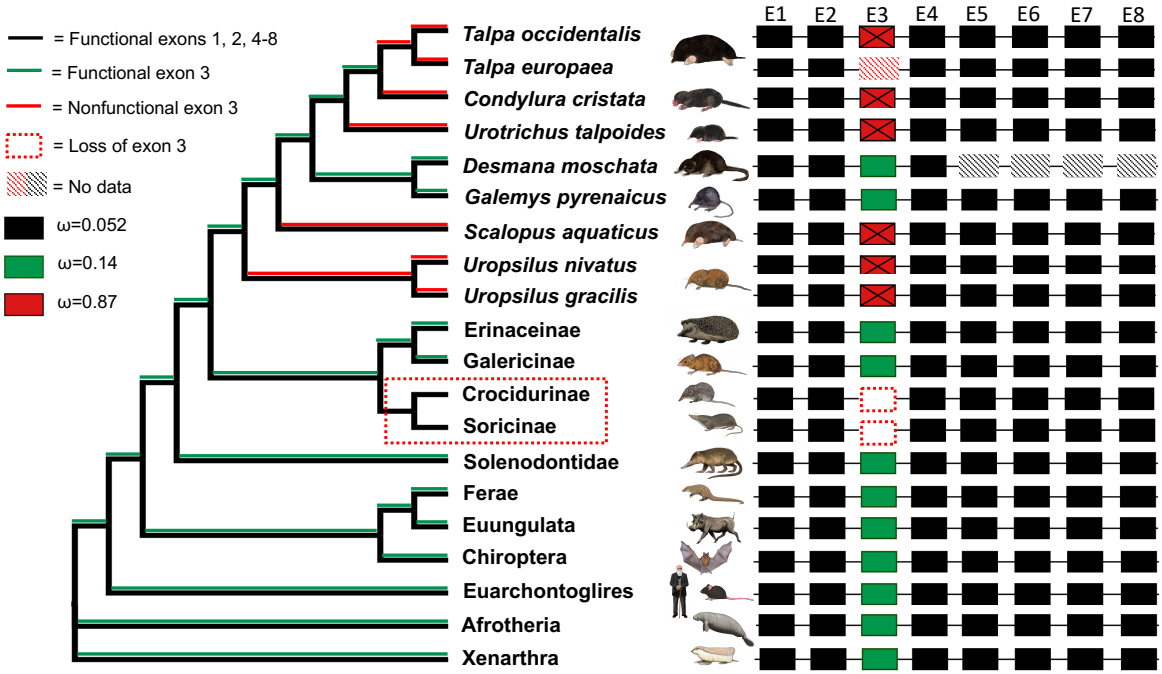

Figure 3.

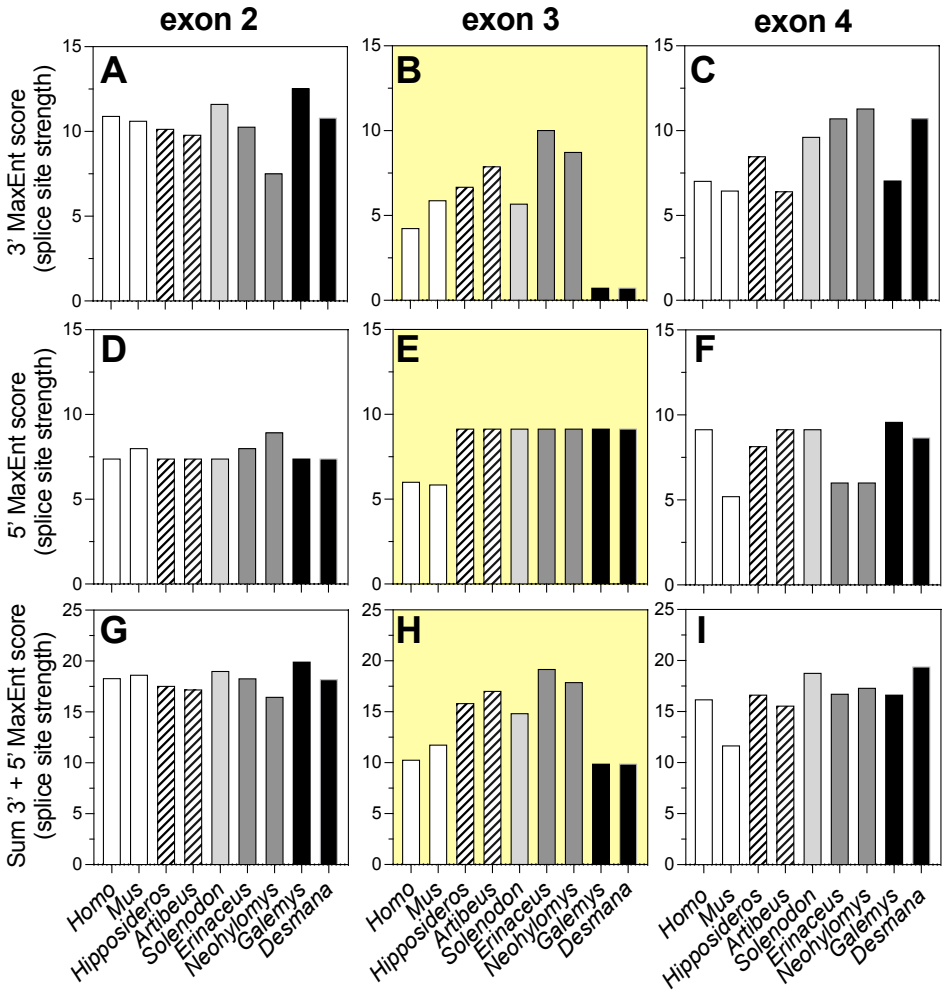

Figure 4.